

Toward pressure-induced multiferroicity in PrMn_2O_5 W. Peng,¹ V. Balédent,¹ S. Chattopadhyay,^{2,3} M.-B. Lepetit,^{4,5} G. Yahia,^{1,6} C. V. Colin,^{4,7} M. J. Gooch,⁸ C. R. Pasquier,¹ P. Auban-Senzier,¹ M. Greenblatt,⁹ and P. Foury-Leylekian^{1,*}¹*Laboratoire de Physique des Solides, CNRS, Université Paris-Sud, Université Paris-Saclay 91405 Orsay cedex, France*²*Université Grenoble Alpes, INAC-MEM, F-38000 Grenoble, France*³*CEA-Grenoble, INAC-MEM, F-38000 Grenoble, France*⁴*CNRS, Institut NEEL, F-38000 Grenoble, France*⁵*Institut Laue Langevin, 72 av. des Martyrs, 38042 Grenoble France*⁶*Laboratoire de Physique de la Matière Condensée, Université Tunis-El Manar, 2092 Tunis, Tunisia*⁷*Université Grenoble Alpes, Institut NEEL, F-38000 Grenoble, France*⁸*Texas Center of Superconductivity, University of Houston, Texas, USA*⁹*Department of Chemistry and Chemical Biology, Rutgers, the State University of New Jersey, Piscataway, New Jersey 08854, USA*

(Received 16 February 2017; published 11 August 2017)

The series of multiferroics RMn_2O_5 is extensively studied for its quasicollinear spin arrangement, which results in an electrical polarization according to the exchange-striction model. Variations of the interatomic distances modified by the external pressure can strongly influence the multiferroic properties. Understanding this influence is of great importance, especially for the future realization of multiferroic devices. As PrMn_2O_5 is paraelectric at ambient pressure, it is the most suitable candidate to search for pressure induced multiferroicity. In this paper, we report the emergence of a new pressure induced magnetic phase in PrMn_2O_5 determined by powder neutron diffraction under pressure. This new magnetic phase presenting at relatively low pressure becomes completely exclusive at 8 GPa. The determination of its magnetic structure has thus been possible for the first time. More importantly, the magnetic structure stabilized under pressure should induce a strong spontaneous electric polarization due to the nearly perfect collinearity of the Mn^{3+} and Mn^{4+} spins.

DOI: [10.1103/PhysRevB.96.054418](https://doi.org/10.1103/PhysRevB.96.054418)**I. INTRODUCTION**

Multiferroicity is one of the hottest topics of investigation in condensed matter physics. Such property, characterized by the simultaneous presence of different coupled orders, gives birth to exceptional multifunctional materials. In particular, magnetoelectric multiferroics can respond to the application of both electric and magnetic fields, and thus can allow a much greater degree of control for electronic devices [1]. For many applications such as data storage, the strength of the magnetoelectric coupling (MEC) is a key element. The design of such materials requires a comprehensive understanding of the relevant parameters influencing this coupling and a microscopic mechanism to explain how they couple to it. In particular, the evolution under external parameters (electric or magnetic field, pressure) may reveal a hidden potential in certain materials such as RMn_2O_5 .

Pursuing that goal, numerous theoretical and experimental studies have been carried out in manganites (mainly in the RMnO_3 and RMn_2O_5 families, where R denotes either a rare earth or Y), including the influence of the temperature [2], the nature of the rare earth [2–4], and the effect of the external magnetic field [5]. The universal feature drawn for these compounds is the presence of a complex magnetic order, originating from a frustration among competing superexchange interactions. This order is also responsible for the emergence of the electric polarization. Since small variations of the interatomic distances directly modify the superexchange integrals, one can expect the multiferroic properties to be strongly

affected by the external pressure. This interesting approach has recently been used on TbMnO_3 , for which a strong increase of the spin-driven polarization has been reported under pressure [6]. A similar effect has been observed (polarization measurements under pressure) in the RMn_2O_5 compounds, with $R=\text{Tb}$, Ho , and Y [7,8]. This result has been ascribed to a new pressure induced magnetic phase in YMn_2O_5 [9,10].

The case of the RMn_2O_5 series is of particular interest since this family demonstrates several prominent properties: (i) a very strong MEC, able to flip the polarization by the application of a small magnetic field [11,12], (ii) an electric polarization among the strongest in magneto-electric multiferroics ($3600 \mu\text{C} \cdot \text{cm}^{-2}$) [13], and (iii) the presence of nonferroelectric members in the series ($R=\text{La}$ and Pr [3]). Moreover, the mechanism responsible for the spin induced ferroelectricity in all the series has recently been definitively clarified. The standard Dzyaloshinskii-Moriya model, which is only compatible with noncollinearly ordered spins, has been ruled out because the RMn_2O_5 series presents a quasicollinear spin arrangement and yet a huge magnetoelectric effect [12]. An exchange-striction model based on the optimization of the frustrated exchange interactions via polar atomic displacements, initially proposed by Chapon [14], has been recently definitively established [15]. The electric polarization can be seen as proportional to the scalar product of the spins involved in the released exchange interactions. It is thus maximum for commensurate magnetic orders and collinear spins. This property explains the decrease of polarization seen in the RMn_2O_5 compounds, at the low-temperature commensurate-to-incommensurate transition [14]. The knowledge of the microscopic mechanism for the MEC allows the prediction of dielectric properties from the magnetic structure.

*Corresponding author: pascale.foury@u-psud.fr

In this paper, we report an accurate determination of the magnetic structure under pressure in PrMn_2O_5 . From powder neutron diffraction experiments under pressure at low temperature, we show that a new magnetic phase develops at high pressure (PCM phase). This new pressure induced magnetic phase exhibits a similar order (same propagation wave vector) as the one reported in YMn_2O_5 and TbMn_2O_5 [9]. Our work thus confirms the universal character of the high-pressure magnetic phase diagram in this family. The scenario of PrMn_2O_5 is, however, much more remarkable. Indeed, not only the compound is nonferroelectric at ambient pressure but also the new phase emerges at very low pressure and is totally stabilized at 8 GPa. This allowed us to perfectly determine the low-temperature and high-pressure magnetic structure. Using an exchange striction model we evidence that PrMn_2O_5 undergoes a pressure-induced transition most probably toward multiferroicity.

The structure of the RMn_2O_5 compounds is composed of chains of Mn^{4+}O_6 octahedra running along the c axis, separated by layers of R^{3+} ions or Mn^{3+}O_4 bipyramids (represented in Fig. 5). In these systems, the magnetic interactions are within the (a,b) plane, in which two zig-zag chains of Mn^{4+}O_6 octahedra and Mn^{3+}O_4 pyramids run along the a axis and are stacked along the b direction. In this plane, there are three inequivalent magnetic super-exchange interactions between Mn ions: J_3 and J_4 for the $\text{Mn}^{3+}\text{-Mn}^{4+}$ couples, and J_5 between two Mn^{3+} spins. Within the chains, the J_5 and J_4 interactions induce an antiferromagnetic (AFM) character of the zigzag chains, while the J_3 couplings between the chains essentially annihilate each other (magnetic frustration). Along the c axis, there are two different AFM $\text{Mn}^{4+}\text{-Mn}^{4+}$ exchange interactions, depending on whether it is the Mn^{3+} (J_2) or R^{3+} (J_1) ions in between the Mn^{4+} layers. In the first case, a strong magnetic frustration appears since there are two J_4 and two J_3 $\text{Mn}^{4+}\text{-Mn}^{3+}$ interactions competing with J_2 . It results in an effective interaction between the two Mn^{4+} ions that is always ferromagnetic (FM) [16,17]. For J_1 , it is more complex and strongly depends on the rare earth (its magnetism and number of $4f$ electrons) as well as on the detailed structural parameters. In particular, it is greatly affected by the distances and angles between cations and oxygens involved in the super-exchange couplings.

At ambient pressure, all RMn_2O_5 , for R heavier than Sm, show similar behaviors, characterized by successive AFM orderings below 40 K, with a propagation vector of the type $\mathbf{q} = (0.5 - \delta, 0, 0.25 + \epsilon)$ varying upon the temperature and the nature of R^{3+} . Concomitantly to a lock-in incommensurate-to-commensurate magnetic transition at ~ 35 K, the ferroelectricity appears and the electric polarization increases upon decreasing temperature. Below a new commensurate-to-incommensurate magnetic transition at ~ 25 K, the polarization usually decreases. At low temperature, an additional magnetic transition stabilizes in certain members of the series, usually attributed to the R^{3+} moments ordering. The compounds with larger R^{3+} size such as $R=\text{La}$ and Pr are not ferroelectric and show commensurate magnetic orderings [3,18]. Surprisingly, in the particular case of PrMn_2O_5 , the first magnetic transition, which occurs at $T_1 = 25\text{K}$, corresponds to the ordering of the Mn^{3+} spins only with a propagation wave vector $\mathbf{q}_1 = (0.5, 0, 0)$ (CM1 phase). Below $T_2 = 20$ K, the Mn^{4+} moments

order (CM2 phase) with a propagation wave vector $\mathbf{q}_2 = (0, 0, 0.5)$. In both phases, a partial order of various components of the Pr^{3+} spins is observed. It is important to notice that the particular value of the propagation wave vector $\mathbf{q}_1 = (0.5, 0, 0)$, is probably not the origin of the nonferroelectric character of PrMn_2O_5 because such propagation wave vector is also observed in the low-temperature phase of DyMn_2O_5 , which presents an electric polarization [19]. In PrMn_2O_5 , the Mn spins are strongly noncollinear to each other and the absence of ferroelectricity can be understood in the exchange-striction model framework.

II. EXPERIMENTAL MEASUREMENTS

The measurements presented in this paper were performed using high-purity polycrystalline samples of PrMn_2O_5 synthesized from a precursor-based flux, following a method described in Refs. [3,18]. Neutron powder diffraction experiments were carried out on the D1B diffractometer (CRG, CNRS ILL-Grenoble, France). The neutron wavelength was 2.52 Å. The pressure setup was a Paris-Edinburgh pressure cell with a sample volume of about 50 mm³. The pressure on the sample volume has been estimated by the calibration of the He-gas pressure on the cell's piston. The pressure cell was inserted in a closed-circle He cryocooler. Measurements were performed by heating up from 6 to 70 K at 3, 5, 7, and 8 GPa. Refinements of the nuclear and magnetic structures were performed using the FULLPROF program [20]. High-pressure dielectric and polarization measurements were measured along the b axis out on a relatively small plate like a single crystal of PrMn_2O_5 , which was placed in a beryllium copper clamp cell capable of hydrostatic pressure up to 18 kbars. Fluorinert FC 70 was used as the pressure medium and pressure was measured *in situ* using a lead manometer in conjecture with a low-frequency (19 Hz) LR700 Inductance Bridge (Linear Research) [21]. Temperature control for both the dielectric and polarization measurements were at a rate of 1–2 K/min. Capacitance was measured at a frequency of 1 kHz with an Andeen-Hagerling capacitance bridge (AH 2500A). While both the real (energy stored) and imaginary (loss factor) capacitances were measured, the real part was used to calculate the dielectric constant and the loss was to assist in data analysis. Pyroelectric current measurements were performed with a Keithley electrometer (K6517A) with a small poling voltage applied on cooling runs and by integrating the pyroelectric current, the polarization was estimated.

III. RESULTS

A. Electric properties

The dielectric constant as a function of temperature for various pressures from 0 to 1.46 GPa was measured on a small single crystal synthesized according to Ref. [3]. The result is shown in Fig. 1. The ambient pressure curve is similar to the one published in Refs. [3,22] at the difference that here, a clear peak shape is visible at 18 K followed by a broader peak at 10 K. These two features recall the one observed in TbMn_2O_5 and attributed to the ferroelectric transition and the electromagnon, respectively. This can be the indication of a ferroelectriclike behavior in PrMn_2O_5 with an electric polarization too small to be detected. Under pressures above

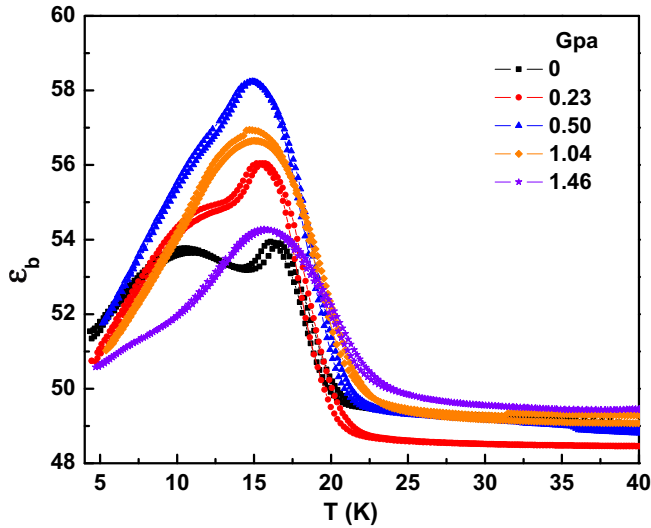


FIG. 1. Dielectric constant measurement as a function of temperature under various pressures (warming and cooling).

0.23 GPa, the two peaks merge into a broad one located at 15 K. The amplitude of this peak first increases to reach a maximum at 0.5 GPa. Above 0.5 GPa, the amplitude of the dielectric constant decreases and joins the ambient pressure value. This can be related to the low-temperature CM2 phase, which is suppressed gradually under pressure. Electric polarization measurements under pressure were attempted. However, no significant signal has been measured even at the highest pressures (1.46 GPa). It is important to notice that in the case of NdMn₂O₅, which has been recently discovered to be ferroelectric [4], the co-alignment of several single crystals were necessary due to very small value of pyroelectric current.

B. Refinement and symmetry analysis

At 3 GPa, below a temperature very close to T_1 , the neutron powder diffraction (NPD) pattern shows ten new magnetic

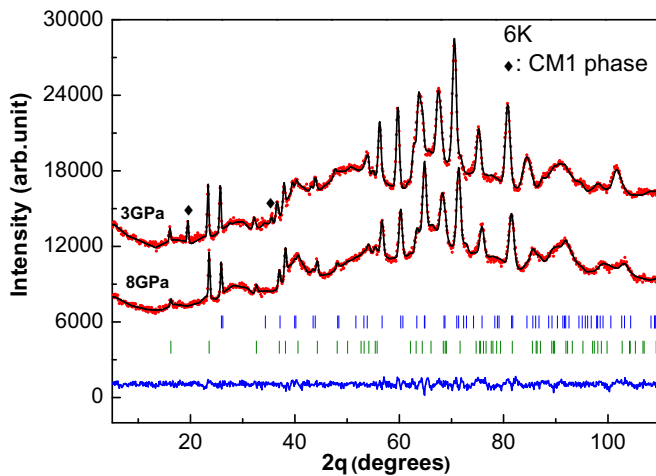


FIG. 2. Rietveld refinement of the neutron diffraction data of PrMn₂O₅ at 6 K, 3 and 8 GPa. The experimental data are in red, the calculated profile in black, and their difference in blue. The diamond symbols indicate the CM1 magnetic reflections. The green bars refer to the nuclear (blue ticks) and PCM phase (green ticks) reflections.

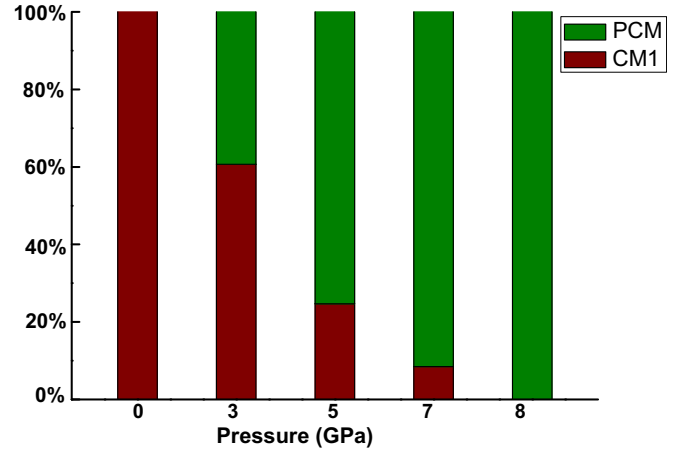


FIG. 3. Evolution as a function of pressure of the ratio between ambient pressure CM1 and pressure induced PCM magnetic phases in PrMn₂O₅ at 6 K.

reflections (see Fig. 2) in addition to the reflections observed at ambient pressure [$\mathbf{q}_1 = (0.5, 0, 0)$]. They are well indexed by the propagation wave vector $\mathbf{q}_{\text{PCM}} = (0.5 \ 0 \ 0.5)$, a result similar to the one observed under pressure in YMn₂O₅ [9]. By further cooling down below T_2 , no additional reflections are observed. This indicates that the lower CM2 phase disappears within the 0 to 3 GPa pressure range. At 5 GPa, the intensity of the $\mathbf{q}_1 = (0.500)$ reflections is strongly reduced at the benefit of the $\mathbf{q}_{\text{PCM}} = (0.5 \ 0 \ 0.5)$ reflections and the critical temperature of the PCM phase is $T_{\text{PCM}} = 30.5$ K. At 7 GPa, the PCM phase appears at $T_{\text{PCM}} = 37.5$ K and the CM1 phase has nearly disappeared from the diffractogram. Finally, at 8 GPa, this PCM phase becomes completely exclusive at $T_{\text{PCM}} = 43$ K. The pressure variation of the ratio between the intensities of the PCM reflections over CM1 ones is represented in Fig. 3. It evidences a competition between both magnetic orders in the 0–8 GPa pressure range with a complete stabilization of the PCM phase at 8 GPa. The pressure-temperature phase diagram of PrMn₂O₅ shown in Fig. 4 is constructed from the neutron diffraction data under pressure. Since there is no solid evidence

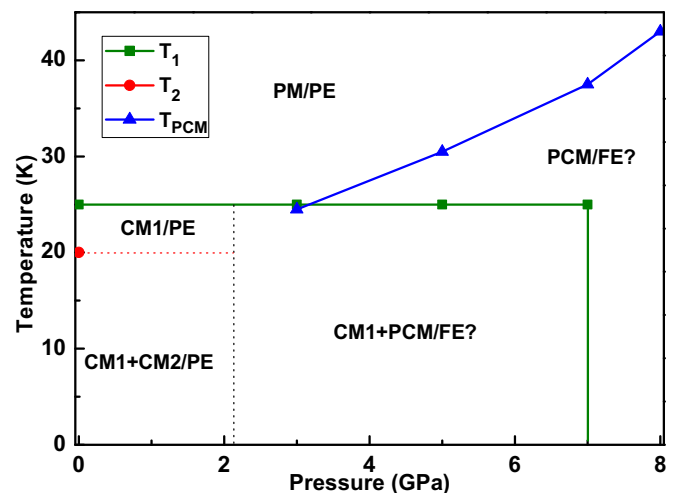


FIG. 4. Pressure-temperature phase diagram of PrMn₂O₅. The lines are a guide to the eye.

of the presence of ferroelectric phase, so we indicate that the phase can be ferroelectric (FE?).

The diffractogram of the new PCM phase has been analyzed at the lowest temperature and highest pressure (6 K, 8 GPa) at which the PCM phase is totally developed and is the only magnetic phase. The structure has been determined by Rietveld refinement, using symmetry considerations derived from representation analysis. Slight deviations from the average structure of $Pbam$ space group have been observed in Ref. [23], the real space group is Pm . Since Pr is located on the m plane, its spin-orbit operator does not commute with the m operation and thus the magnetic space group commuting with the system Hamiltonian can only be Pm' . The $\mathbf{q}_{PCM} = (0.5\ 0\ 0.5)$ propagation vector corresponds to the D point of the Brillouin zone. There are two irreducible representations (irrep) at this point, D_1 and D_2 . In the D_1 irrep, the Mn^{3+} magnetic moments are compelled to be along the c direction, while the Pr^{3+} ones are in the (a, b) plane. In the D_2 irrep, it is the reverse. No specific orientation of the Mn^{4+} magnetic moments is imposed by the symmetry. In a spin-orbit plus crystal field atomic model, the ground-state of the Pr^{3+} ion, a non-Kramers ion, is in a nondegenerate one-dimensional co-representation of its spin-electronic structure, and as a consequence, its magnetic moment is null. Nonzero Pr magnetic moments can only arise from the hybridization of the Pr $4f$ orbitals with the neighboring atoms. We therefore initially neglected the Pr contribution in our refinement. In order to reduce the number of degrees of freedom, we enforced pairing arising from the weakly broken symmetries of the $Pbam$ space group. We have also considered that identical ions have the same moments.

The best refinement is obtained when all spins lie nearly parallel to the a axis (D_2 representation). The magnetic structure is characterized by a ferromagnetic arrangement along c for the Mn^{4+} spins belonging to the same unit cell, and an AFM arrangement between neighboring unit cells (see Fig. 5). For Mn^{3+} , there is an antiferromagnetic pairing relating the moments at (x, y, z) and $(-x, -y, z)$ and a ferromagnetic arrangement relating the spins at $(-x + 1/2, y + 1/2, -z)$ and $(x + 1/2, -y + 1/2, -z)$. Note that the refinement is not improved when one introduces a partial order of the Pr^{3+} . The magnetic ordering at 8 GPa and 6 K is illustrated in Fig. 5 and given in Table I. The ordered moments of the Mn^{3+} and Mn^{4+} are very similar and quasialigned along the a direction. Looking now at the symmetry operations leaving this magnetic

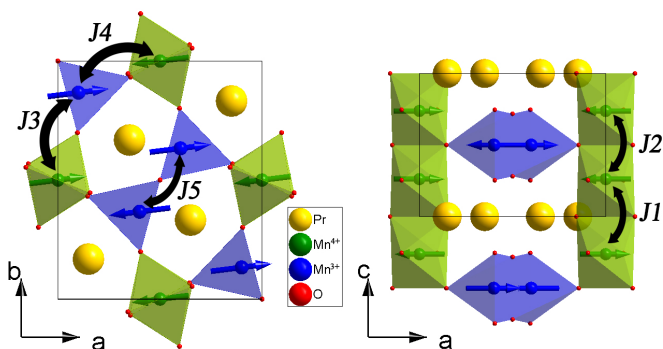


FIG. 5. Magnetic structure of $PrMn_2O_5$ at 6 K and 8 GPa. Black arrows denote the five super-exchange couplings.

TABLE I. Magnetic structure parameters of $PrMn_2O_5$ at 6 K and 8 GPa. α is the angle between the a axis and the magnetic moment.

	x/a	y/b	z/c	α	μ_B
Mn^{3+}	0.399(69)	0.366(98)	0.5	5(017)	2.8(22)
Mn^{4+}	0	0.5	0.262(10)	5(015)	2.6(39)

structure invariant, we find the following generators issued from the $Pbam$ crystallographic group $\{E, m, 2'_1, b', t'_a, t'_c\}$. This is the $Pmc'2'_1$ magnetic space group according to the Bilbao Crystallographic server [24,25] (BNS and OG setting).

IV. DISCUSSION AND CONCLUSION

The effect of pressure on the magnetic structure of $PrMn_2O_5$ is very similar to the one previously observed in YMn_2O_5 [9] with the appearance of a new PCM phase with $\mathbf{q}_{PCM} = (0.5\ 0\ 0.5)$. This feature is thus likely to be a universal property of the RMn_2O_5 series under pressure. However, this new PCM phase is much better stabilized in $PrMn_2O_5$. Firstly, at 3 GPa, the $(0.5\ 0\ 0.5)$ magnetic reflection exhibits the largest intensity in the series and secondly, the CM1 phase has completely disappeared at 8 GPa in $PrMn_2O_5$, while it still exists with a proportion of 70% in YMn_2O_5 [9]. Finally, the strong increase of T_{PCM} with pressure in the Pr compound is the fingerprint of exceptional stability at high pressure. Thus $PrMn_2O_5$ is an outstanding model to investigate the high-pressure multiferroic properties.

It is important to understand the origin of the stabilization of the PCM phase under pressure. Let us first consider the propagation wave vector and in particular its c^* component. As previously mentioned, the order along c is related to the interaction between Mn^{4+} , either through the J_1 exchange interaction or through the R^{3+} (the ordering related to J_2 always being FM due to magnetic frustration). For nonmagnetic R^{3+} such as La [26] and Bi [27], the only contribution is J_1 ($Mn^{4+}-O^2--Mn^{4+}$), which is AFM. The same scenario can be expected for R^{3+} with an even number of $4f$ electrons, such as Pr^{3+} , because the R^{3+} magnetic moment is expected to be close to nil as seen previously. At ambient pressure two quasidegenerate ground states (one only on the Mn^{3+} and Pr^{3+} ions, and the other only on the Mn^{4+} ones) are stabilized [3], with orthogonal (and thus no coupling) directions for the two Mn subsystems. The coupling between the Mn^{3+} and Mn^{4+} subsystems is controlled by the J_4 parameter which is strongly dependent on the $Mn_1-O_3-Mn_2$ angle [16]. However, as shown in Fig. 6 for the Pr composition and as observed in Y, Bi, and Ho [10,28], the a lattice parameter strongly decreases with pressure. This induces a decrease of the angle involved in J_4 (from 132.5° at 0 GPa to 130.5° at 8 GPa) with increasing pressure. J_4 should thus increase in absolute value. As a result, the coupling between the Mn^{4+} and Mn^{3+} subsystems increases and the energy of the PCM state decreases below the energy of the two ambient pressure lowest energy states.

In the light of our recent result validating the exchange striction mechanism for the RMn_2O_5 series [15], the quasico-linear spin alignment in the PCM phase has a major

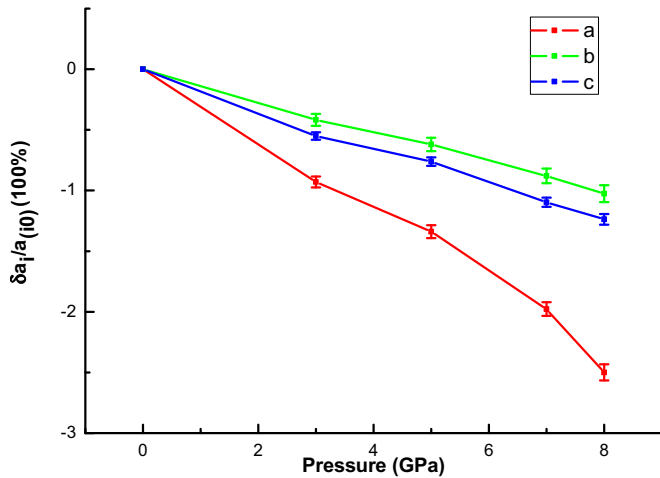


FIG. 6. Relative pressure dependence of the unit cell parameters ($a_i - a_{i0}/a_{i0}$) of PrMn₂O₅ with respect to their ambient pressure values at 6 K. a_{i0} is a unit cell parameters under ambient pressure at 6 K.

consequence on the dielectric properties. Indeed, in this model, the electric polarization magnitude is proportional to the scalar product of the spins connected through J_3 . This explains why the noncollinear spin arrangement of PrMn₂O₅ at low pressure leads to the absence of ferroelectricity. However, this mechanism also indicates that the collinear commensurate phase of PrMn₂O₅ at 8 GPa should exhibit a high electric polarization as all spins are collinear. Dielectric constant

and electric polarization measurements are very difficult in the range of pressures that we have investigated, but the measurements have been performed at low pressure. As expected the dielectric constant is strongly modified under pressure. However, its behavior is more complex as expected. Indeed, after a first increase, we observe that the dielectric constant decreases to reach values close to the ambient pressure at 1.46 GPa. As for the calculation of the electric polarization in the PCM phase, it is also very difficult requiring an accurate crystallographic structure refined in a noncentrosymmetric space group. Such an accuracy is not reachable using the neutron powder diffraction data we have.

In conclusion, we reported a new magnetic phase that developed at high pressure in PrMn₂O₅. This new phase is likely to be common to the RMn₂O₅ series, as it is similar to the one reported in $R=Y$ and Tb. Further studies on other members are required to definitely confirm this universal character. The most remarkable feature of PrMn₂O₅ under pressure is that the Mn spins become collinear, which is expected to induce ferroelectricity according to the exchange striction model. This presages a pressure induced multiferroic transition in the nonferroelectric PrMn₂O₅ and paves the way to the conception of new multiferroic materials with tunable properties.

ACKNOWLEDGMENTS

This work was supported by the Chinese Scholarship Council project. The work of M. Greenblatt at Rutgers was supported by NSF-DMR 15040976 grant.

-
- [1] W. Eerenstein, N. D. Mathur, and J. F. Scott, *Nature (London)* **442**, 759 (2006).
- [2] G. R. Blake, L. C. Chapon, P. G. Radaelli, S. Park, N. Hur, S. W. Cheong, and J. Rodríguez-Carvajal, *Phys. Rev. B* **71**, 214402 (2005).
- [3] C. Doubrovsky, G. André, A. Gukasov, P. Auban-Senzier, C. R. Pasquier, E. Elkaim, M. Li, M. Greenblatt, F. Damay, and P. Foury-Leylekian, *Phys. Rev. B* **86**, 174417 (2012).
- [4] S. Chattopadhyay, V. Balédent, F. Damay, A. Gukasov, E. Moshopoulou, P. Auban-Senzier, C. Pasquier, G. André, F. Porcher, E. Elkaim, C. Doubrovsky, M. Greenblatt, and P. Foury-Leylekian, *Phys. Rev. B* **93**, 104406 (2016).
- [5] W. Ratcliff, V. Kiryukhin, M. Kenzelmann, S. H. Lee, R. Erwin, J. Schefer, N. Hur, S. Park, and S. W. Cheong, *Phys. Rev. B* **72**, 060407 (2005).
- [6] N. Terada, D. D. Khalyavin, P. Manuel, T. Osakabe, A. Kikkawa, and H. Kitazawa, *Phys. Rev. B* **93**, 081104 (2016).
- [7] C. R. dela Cruz, F. Yen, B. Lorenz, M. M. Gospodinov, C. W. Chu, W. Ratcliff, J. W. Lynn, S. Park, and S. W. Cheong, *Phys. Rev. B* **73**, 100406 (2006).
- [8] R. P. Chaudhury, C. R. dela Cruz, B. Lorenz, Y. Sun, C.-W. Chu, S. Park, and Sang-W. Cheong, *Phys. Rev. B* **77**, 220104(R) (2008).
- [9] M. Deutsch, T. C. Hansen, M. T. Fernandez-Diaz, A. Forget, D. Colson, F. Porcher, and I. Mirebeau, *Phys. Rev. B* **92**, 060410 (2015).
- [10] D. P. Kozlenko, N. T. Dang, S. E. Kichanov, E. V. Lukin, A. M. Pashayev, A. I. Mammadov, S. H. Jabarov, L. S. Dubrovinsky, H. P. Liermann, W. Morgenroth, R. Z. Mehdiyeva, V. G. Smotrakov, and B. N. Savenko, *Phys. Rev. B* **92**, 134409 (2015).
- [11] N. Hur, S. Park, P. Sharma, J. Ahn, S. Guha, and S.-W. Cheong, *Nature (London)* **429**, 392 (2004).
- [12] I. A. Sergienko and E. Dagotto, *Phys. Rev. B* **73**, 094434 (2006).
- [13] N. Lee, C. Vecchini, Y. J. Choi, L. C. Chapon, A. Bombardi, P. G. Radaelli, and S. W. Cheong, *Phys. Rev. Lett.* **110**, 137203 (2013).
- [14] L. C. Chapon, G. R. Blake, M. J. Gutmann, S. Park, N. Hur, P. G. Radaelli, and S. W. Cheong, *Phys. Rev. Lett.* **93**, 177402 (2004).
- [15] G. Yahia, F. Damay, S. Chattopadhyay, V. Balédent, W. Peng, E. Elkaim, M. Whitaker, M. Greenblatt, M.-B. Lepetit, and P. Foury-Leylekian, *Phys. Rev. B* **95**, 184112 (2017).
- [16] S. Petit, V. Balédent, C. Doubrovsky, M. B. Lepetit, M. Greenblatt, B. Wanklyn, and P. Foury-Leylekian, *Phys. Rev. B* **87**, 140301 (2013).
- [17] P. G. Radaelli and L. C. Chapon, *J. Phys.: Condens. Matter* **20**, 434213 (2008).
- [18] J. Alonso, M. Casais, M. Martínez-Lope, J. Martínez, and M. Fernández-Díaz, *J. Phys.: Condens. Matter* **9**, 8515 (1997).
- [19] Z. Y. Zhao, M. F. Liu, X. Li, L. Lin, Z. B. Yan, S. Dong, and J. M. Liu, *Sci. Rep.* **4**, 3984 (2014).

- [20] J. Rodríguez-Carvajal, *Physica B* **192**, 55 (1993).
- [21] A. Eichler and J. Wittig, *Z. Angew. Phys.* **25**, 319 (1968).
- [22] A. B. Sushkov, R. V. Aguilar, S. Park, S.-W. Cheong, and H. D. Drew, *Phys. Rev. Lett.* **98**, 027202 (2007).
- [23] V. Balédent, S. Chattopadhyay, P. Fertey, M. B. Lepetit, M. Greenblatt, B. Wanklyn, F. O. Saouma, J. I. Jang, and P. Foury-Leylekian, *Phys. Rev. Lett.* **114**, 117601 (2015).
- [24] M. I. Aroyo, J. M. Perez-Mato, D. Orobengoa, E. Tasci, G. de la Flor, and A. Kirov, *Bulg. Chem. Commun.* **43**, 183 (2011).
- [25] S. V. Gallego, E. S. Tasci, G. de la Flor, J. M. Perez-Mato, and M. I. Aroyo, *J. Appl. Cryst.* **45**, 1236 (2012).
- [26] A. Muñoz, J. A. Alonso, M. T. Casais, M. J. Martínez-Lope, J. L. Martínez, and M. T. Fernández-Díaz, *Eur. J. Inorg. Chem.* **2005**, 685 (2005).
- [27] A. Muñoz, J. A. Alonso, M. T. Casais, M. J. Martínez-Lope, J. L. Martínez, and M. T. Fernández-Díaz, *Phys. Rev. B* **65**, 144423 (2002).
- [28] A. Grzechnik, M. Tolkiehn, W. Morgenroth, and K. Friese, *J. Phys.: Condens. Matter* **22**, 275401 (2010).